

## Article

## Adding Crystals to Minimize Clogging in Continuous Flow Synthesis

Gaurav Giri, Lu Yang, Yiming Mo, and Klavs F. Jensen

*Cryst. Growth Des.*, **Just Accepted Manuscript** • DOI: 10.1021/acs.cgd.8b00999 • Publication Date (Web): 27 Nov 2018Downloaded from <http://pubs.acs.org> on December 5, 2018

### Just Accepted

“Just Accepted” manuscripts have been peer-reviewed and accepted for publication. They are posted online prior to technical editing, formatting for publication and author proofing. The American Chemical Society provides “Just Accepted” as a service to the research community to expedite the dissemination of scientific material as soon as possible after acceptance. “Just Accepted” manuscripts appear in full in PDF format accompanied by an HTML abstract. “Just Accepted” manuscripts have been fully peer reviewed, but should not be considered the official version of record. They are citable by the Digital Object Identifier (DOI®). “Just Accepted” is an optional service offered to authors. Therefore, the “Just Accepted” Web site may not include all articles that will be published in the journal. After a manuscript is technically edited and formatted, it will be removed from the “Just Accepted” Web site and published as an ASAP article. Note that technical editing may introduce minor changes to the manuscript text and/or graphics which could affect content, and all legal disclaimers and ethical guidelines that apply to the journal pertain. ACS cannot be held responsible for errors or consequences arising from the use of information contained in these “Just Accepted” manuscripts.



## Adding Crystals to Minimize Clogging in Continuous Flow Synthesis

Gaurav Giri<sup>1,2</sup>, Lu Yang<sup>1</sup>, Yiming Mo<sup>1</sup> and Klavs F. Jensen\*<sup>1</sup>

1 Department of Chemical Engineering, Massachusetts Institute of Technology, Cambridge, MA 02139

2 Department of Chemical Engineering, University of Virginia, Charlottesville, VA 22901

Corresponding Author Email Address: [kfjensen@mit.edu](mailto:kfjensen@mit.edu)

### Abstract:

For many carbon-carbon and carbon-nitrogen bond-forming reactions, the stoichiometric formation of inorganic salt crystals limits continuous flow synthesis by causing precipitation, agglomeration, and ultimately clogging of the reactor. We describe a new method of mitigating uncontrolled clogging by adding crystals into the reactant stream. Adding seed crystals of the inorganic salt byproduct shifts the crystallization from uncontrolled nucleation to controlled heterogeneous growth. Reactions with the addition of high quality crystals show less agglomeration compared to the unseeded reaction. We realize the formation of high quality seeds using multiple methods including filtration and settling. Modelling enables balancing of the reaction rate and deposition of the salt onto seed crystals to prolong reactor operating times without clogging.

### Introduction:

Continuous flow synthesis is well known in production of commodity chemicals, and small scale analogs are finding increasing use in fine chemicals, pharmaceuticals, and nanomaterials under the term, flow chemistry. The enhanced heat and mass transfer rates present in small scale continuous flow systems enable efficient and safe chemical synthesis.<sup>1-7</sup> However, reactions that involve solids present challenges for continuous flow methods. Solids may be present in the reaction as reagents, intermediates, byproducts or as the product.<sup>8-21</sup> In batch systems, forced convective

1  
2  
3 mixing allows the use of solids during reactions. However, lack of convective mixing and the small  
4 reactor cross sectional area in continuous flow systems increases the probability that solids clog  
5 the channel, leading to an early termination of the process. In organic synthesis, numerous  
6 reactions that are pharmaceutically and industrially relevant involve the formation of  
7 stoichiometric amounts of inorganic crystalline salts,<sup>12, 22</sup> which precipitate in organic solvents and  
8 ultimately clog small-scale reactors (with millimeter or submillimeter diameters), sometimes  
9 irreversibly. Minimizing clogging will help open up additional opportunities for continuous flow  
10 synthesis.  
11  
12  
13  
14  
15  
16  
17  
18  
19  
20  
21

22 Numerous methods have been explored to mitigate solid clogging in microreactors, such as  
23 addition of solvents that dissolve salts, use of pressure pulses, application of ultrasonication, or  
24 changing the synthesis to not create solids.<sup>12, 17, 19, 23-25</sup> For example, Buchwald et al. have used a  
25 fluid-fluid biphasic packed bed reactor for C-N cross coupling, where the aqueous portion  
26 dissolved the salt byproduct.<sup>23</sup> However, using secondary fluids only to dissolve salts can reduce  
27 the throughput of the reaction, and care has to be taken to ensure adequate mass transfer rates to  
28 the secondary fluid phase. Changing synthetic conditions can also remove the solid formation  
29 issue, but is harder to generalize across different chemistries. The use of different reactors can also  
30 reduce the impact of solid formation.<sup>26, 27</sup> For example, the use of miniature CSTR cascades can  
31 be used to realize continuous flow production with solid byproducts.<sup>26</sup> Ultrasonication can cause  
32 a rise in the temperature in the reactor, changing the chemical reaction rate.<sup>12</sup> Moreover, these  
33 methods require additional processing equipment, and increase the system complexity. In this  
34 work, we approach the issue of clogging from a conceptually and technically different perspective,  
35 namely, that of crystal engineering.  
36  
37  
38  
39  
40  
41  
42  
43  
44  
45  
46  
47  
48  
49  
50  
51  
52  
53  
54  
55  
56  
57  
58  
59  
60

1  
2  
3 It is well known that the nucleation and growth of crystals is dependent on the supersaturation of  
4 the molecules or ions, and the classical crystallization mechanism has been verified for KCl salt  
5 crystals.<sup>28</sup> The low solubility of KCl in solvents generally used for C-N bond formation reactions  
6 (like tetrahydrofuran) causes a large nucleation rate of KCl crystallites, through homogeneous or  
7 heterogeneous nucleation pathways. However, a competition between nucleation and growth  
8 exists in this system. We hypothesize a proportion of the KCl formed during the reaction can grow  
9 on the KCl seed crystals. This ‘seeding’ technique has been previously utilized to shift  
10 crystallization systems from nucleation to growth in multiple materials, including pharmaceutical  
11 compounds, and inorganic materials.<sup>29-32</sup>

12  
13  
14  
15  
16  
17  
18  
19  
20  
21  
22  
23  
24  
25 The research outlined in this paper involves using this hypothesis to increase reactor lifetime.  
26 Seeded crystal growth to prevent clogging in continuous flow systems has not been explored  
27 before. Instead of avoiding the formation of crystalline solids, we add more solids in the form of  
28 seed crystals to suppress uncontrolled nucleation, and allow for the KCl formed during the reaction  
29 to grow onto the seed crystals. The seed crystals acts as a sink for the inorganic salt produced in  
30 the reaction, resulting in a decreased supersaturation profile, reducing secondary nucleation and  
31 fractal-like crystallites, thereby reducing agglomeration and clogging in the reaction region. We  
32 show the effectiveness of seeded crystallization strategy to reduce clogging during the  
33 pharmaceutically relevant palladium (Pd) catalyzed C-N bond formation reactions. This  
34 effectiveness is shown by both reactor performance, and the morphology of the crystals that are  
35 obtained in typical reactor conditions with and without seeds. Finally, to study the possibility of  
36 whether modelling can be utilized to predict the size and amount of seed crystals that need to be  
37 added into the reactor, a model is developed to balance the salt formation and deposition onto the  
38  
39  
40  
41  
42  
43  
44  
45  
46  
47  
48  
49  
50  
51  
52  
53  
54  
55  
56  
57  
58  
59  
60

1  
2  
3 seeds as a function of reaction conditions and seed crystal number and morphology. **Experimental**

4  
5 **Section:**

6  
7  
8 **Materials:**

9  
10  
11 Aniline, 4-chloroanisole, sublimed grade potassium tert-butoxide (KOtBu), potassium chloride  
12 (KCl), and 2-methyltetrahydrofuran (mTHF) (Sigma-Aldrich Corporation) were used as  
13  
14 purchased. Methylated Brett Phos Palladium catalyst (N-Me-BP-Pd) were prepared according to  
15  
16 literature procedures.<sup>33</sup>  
17  
18

19  
20  
21 **Potassium Chloride Seed Formation:**

22  
23  
24 KCl crystallites with upper size of 35  $\mu\text{m}$  were obtained by grinding KCl powder using a mortar  
25  
26 and pestle, followed by dry sieving using a 35  $\mu\text{m}$  stainless steel mesh sieve (WS Tyler).  
27  
28 Crystallites were suspended in mTHF by continuous stirring at 1600 rpm (Dyla-Dual Hot Plate  
29  
30 Stirrer, VWR International).  
31  
32

33  
34  
35 KCl crystallites with an upper size of 5  $\mu\text{m}$  were obtained by first grinding the KCl as received,  
36  
37 then dry sieving with a 35  $\mu\text{m}$  stainless steel mesh sieve. These crystallites were then suspended  
38  
39 in mTHF. A 5  $\mu\text{m}$  syringe filter (VWR International) was used to isolate KCl crystallites with an  
40  
41 upper size limit of 5  $\mu\text{m}$ . The crystal stock solution was enriched by evaporating mTHF. The  
42  
43 concentration and average size of the crystal seeds were measured by using a Countess II cell  
44  
45 counter (Beckman Coulter Incorporated).  
46  
47

48  
49  
50 KCl crystallites with an upper bound of 7  $\mu\text{m}$  were prepared by using the settling method. The  
51  
52 received KCl were ground using a mortar and pestle and then dry sieved with a 35  $\mu\text{m}$  stainless  
53  
54 steel mesh sieve. These crystallites were suspended in mTHF. After stirring the crystallites at 1600  
55  
56

1  
2  
3 rpm, the crystals were allowed to settle. The settling time was determined such that the top half of  
4  
5 the 40 mL vial would contain crystallites smaller than 7  $\mu\text{m}$ . The top portion of the suspension was  
6  
7 removed gently without disturbing the settled crystals. The crystal solution was enriched by  
8  
9 evaporating mTHF. The crystal size was measured using scanning electron microscopy (SEM).  
10  
11 Sodium Bromide (NaBr) seed crystals were created and characterized using the same method.  
12  
13  
14

15  
16 General procedure for Pd-catalyzed amination reactions:  
17

18  
19 A 20 mL vial with a PTFE screw top cap (VWR International), equipped with a magnetic stirbar,  
20  
21 was charged with dodecane (51.1 mg, 0.1 mmol), aniline (279.4 mg, 3 mmol), 4-chloroanisole  
22  
23 (513.2 mg, 3.6 mmol) and the stock solution of KCl seed crystals (0-1 mL). This solution was  
24  
25 sparged with Argon for 30 min to ensure removal of dissolved Oxygen. Argon-sparged mTHF was  
26  
27 added to bring the final solution volume to 6.0 mL. In another 20 mL vial with a PTFE screw top  
28  
29 cap, the N-Me-BP-Pd catalyst (27.6 mg, 0.03 mmol) was added along with a magnetic stirbar. This  
30  
31 vial was evacuated and backfilled with Argon a total of 3 times. Reagent solution from the first  
32  
33 vial was added to this vial under positive Argon pressure to make up solution 1. This solution was  
34  
35 connected to the reactor using a flow pump (Asia Flow Pump, Syrris).  
36  
37  
38  
39

40  
41 An oven dried vial with a PTFE screw top cap was evacuated and backfilled with Argon, and then  
42  
43 charged with KOtBu (0.505 g, 45 mmol). The vessel was evacuated and backfilled with Argon,  
44  
45 and mTHF was added to bring the final volume of the solution to 6 mL (solution 2). After vigorous  
46  
47 mixing, this solution was loaded into a Normject plastic syringe (10 mL) and filtered through a  
48  
49 PTFE membrane filter (0.4  $\mu\text{m}$  porosity, VWR International) into an oven dried 20 mL vial with  
50  
51 a PTFE screw top cap that had been purged with argon. Solution 2 was then loaded into a stainless  
52  
53 steel syringe (8 mL, Harvard Apparatus). This system was connected to the reactor.  
54  
55  
56  
57  
58  
59  
60

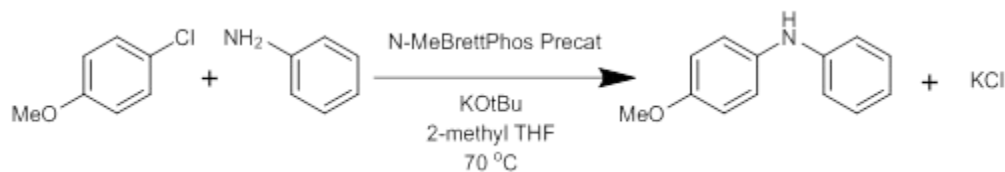
1  
2  
3 A Teflon reactor (perfluoroalkoxy alkane (PFA), 1/16" OD x 0.04" ID x 3' - 6' IDEX Corporation)  
4 was inserted into a spiral aluminum frame (Proto Labs) and heated to the specified temperature  
5 (60 - 90 °C) on a hot plate (VWR International). All fluidic connects were made using ¼ in.-28  
6 PTFE fittings. Flowrate and pressures were allowed to stabilize to a steady state (3 reactor  
7 volumes) and a sample was collected for the duration of the experiment. The product stream was  
8 collected under argon, into water or mTHF. An aliquot of the organic layer was mixed in a vial  
9 containing water, KCl and ethyl acetate. The organic layer from this vial was isolated and run in a  
10 gas chromatography (GC) system (6890 Series, Agilent Technologies). Sample yields were  
11 measured by GC analysis of the organic layer, relative to the dodecane internal standard. Mass  
12 spectroscopy of the product showed the product to be 4-methoxy-N-phenylaniline.<sup>12</sup>  
13  
14  
15  
16  
17  
18  
19  
20  
21  
22  
23  
24  
25

26  
27 Optical characterization and scanning electronic microscopy (SEM):  
28  
29

30 Optical characterization of the crystal seeds were performed using the Countess II Cell Counter  
31 (Beckman Coulter Incorporated). 10 µL of the stock solution of KCl crystal seeds were loaded  
32 onto a cell counter chip. SEM characterization of the crystal seeds required loading and drying 100  
33 µL of the crystal seed stock solution as a uniform layer onto 1 cm<sup>2</sup> carbon tape attached on a sample  
34 pin. The samples were measured on the Zeiss Merlin High Resolution SEM (Zeiss). To  
35 characterize the KCl byproduct after the reaction, 100 µL of the reaction solution was diluted in  
36 900 µL mTHF, and 100 µL of the diluted solution was loaded onto 1 cm<sup>2</sup> carbon tape attached on  
37 a sample pin. Evaporation of Au (5-10 nm) on the samples ensured a conductive layer for ease of  
38 imaging.  
39  
40  
41  
42  
43  
44  
45  
46  
47  
48  
49  
50

51 **Results and Discussion:**  
52  
53  
54  
55  
56  
57  
58  
59  
60

1  
2  
3 The Pd-catalyzed C-N bond forming reaction is widely pursued in the production of intermediates,  
4 active pharmaceutical ingredients (API), and natural products.<sup>34-37</sup> We study the coupling of  
5 aniline and 4-chloroanisole using a Pd catalyst, with the N-Me-Brett Phos ligand, to form 4-  
6 methoxy-N-phenylaniline as the product (**Scheme 1**).<sup>38</sup> This reaction produces a stoichiometric  
7 amount of salt as byproduct, in this case, potassium chloride (KCl). KCl is insoluble in 2-  
8 methyltetrahydrofuran (mTHF), the solvent used to carry out the reaction. The reaction is complete  
9 in minutes, resulting in fast rates of salt formation, which can easily clog microfluidic or  
10 millifluidic systems utilized in continuous flow synthesis.<sup>13, 17, 26</sup>



**Scheme 1: Pd-catalyzed amination of an aryl chloride with aniline.**

33 A single-phase tube-based continuous flow system is employed to study clogging of this reaction.  
34 In a typical experiment, the reagents aniline and 4-chloroanisole, along with the catalyst N-Me-  
35 BP-Pd, are delivered to the reactor using a syringe pump, and the base KOtBu is delivered from a  
36 stainless steel syringe driven by a syringe pump (**Figure 1**). The reagent streams are mixed in a T-  
37 junction and are delivered to a heated reactor. The sample is then collected in a vial downstream.  
38  
39  
40  
41  
42  
43  
44  
45  
46  
47  
48  
49  
50  
51  
52  
53  
54  
55  
56  
57  
58  
59  
60

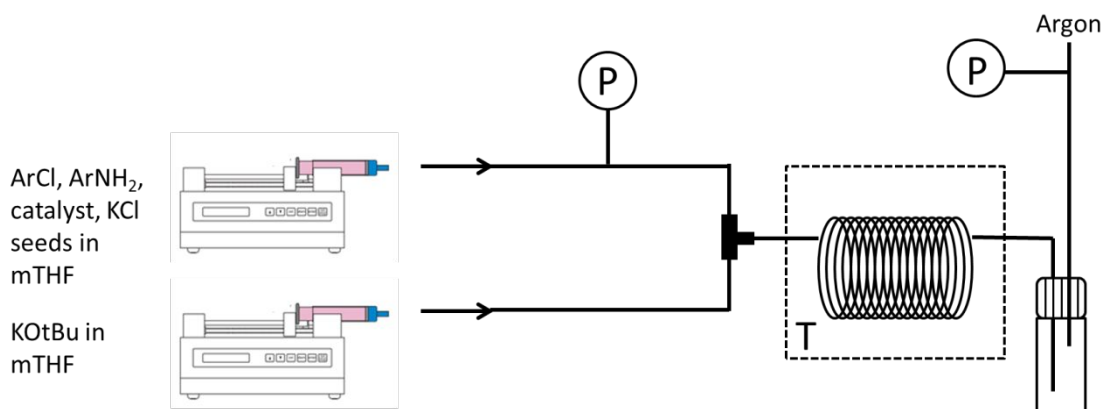


**Figure 1: Experimental setup used to carry out the flow chemistry and clogging experiments.**

In our strategy, adding crystal seeds of the salt increases the rate of crystal growth due to the increased surface area, while having the additional benefit of lowering supersaturation, and thus lowering the rate of crystal nucleation.<sup>39</sup> SEM of a representative product stream after dilution and drying shows different salt crystal morphologies with and without crystal seeds present in the reaction. In the control reaction without seeds, fractal-like KCl crystal morphology is observed (**Figure 2a**). We hypothesize that the high degree of supersaturation that occurs during the reaction causes uncontrolled nucleation of numerous KCl crystallites, which then aggregate to form fractal structures.<sup>40, 41</sup> These structures have a larger surface area per unit mass compared to compact KCl crystals, leading to more inter-particle collisions and interactions. The combination of numerous secondary crystallites and increased interactions leads to larger agglomerates<sup>42</sup>, which causes flow resistance in the continuous flow system, eventually resulting in clogging.

In contrast, the initial seeds added in the reaction stream serve as a sink for the KCl produced during the reaction, and lead to a shift of the KCl crystal morphology from a fractal-like system to a more compact structure (**Figure 2b**). As the KCl growth onto the seed crystals creates relatively compact structures, aggregation of KCl is reduced compared to the control reaction, even if the

total mass of KCl produced is the same. Lowered aggregation leads to minimized clogging events in the small scale reactor. Real-time optical observation of the reactor also shows the different crystal morphologies with and without the addition of initial crystal seeds (**Supplementary Video 1, 2**). In the control reaction, collisions between crystallites cause the formation of larger agglomerates (**Figure 2c**). In contrast, the reaction with seed crystals show smaller crystals and aggregated particles, leading to less collisions and agglomeration (**Figure 2d**).

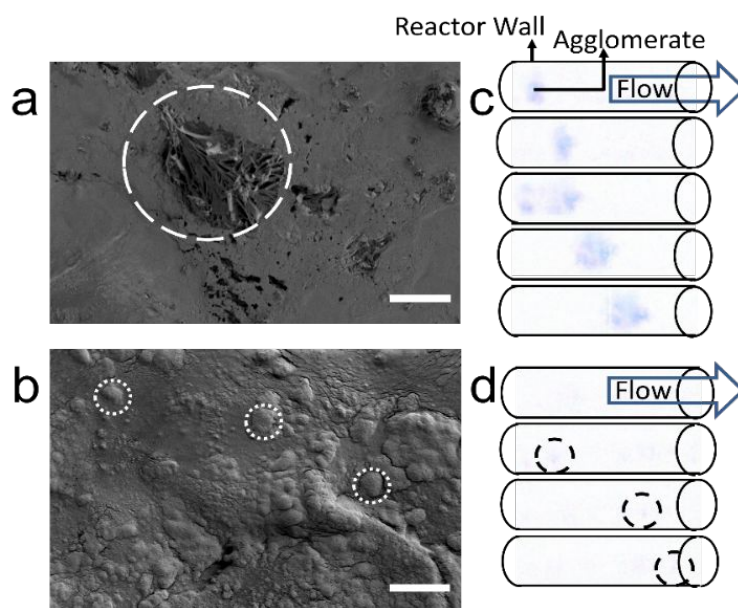


**Figure 2: Scanning electron microscope (SEM) and in situ optical microscope images showing KCl crystal morphology from the reaction stream. (a) Fractal-like morphology observed in reaction stream without crystal seeds. Scale bar is 50  $\mu\text{m}$ . 5-10 nm gold was evaporated on the substrates to obtain contrast and reduce charging. (b) Compact crystallite morphology observed in reaction stream with crystal seeds. Scale bar is 50  $\mu\text{m}$ . 5-10 nm gold was evaporated on the substrates to obtain good contrast. (a),(b) 0.25 M reagents (80  $^{\circ}\text{C}$ , 400  $\mu\text{L}$  flowrate and residence time ( $t_{\text{R}}$ ) = 2 min). (c) In situ optical images show the progression of agglomeration in the reactor. Image was processed for clarity by enhancing the contrast**

1  
2  
3 between the solution and the salt crystals, and removing the solvent color. (d) In-situ optical  
4 image of reaction with seeds, no agglomeration is observed. Small crystals are outlined in the  
5 picture. Image was processed for clarity by enhancing the contrast between the solution and  
6 the salt crystals, and removing the solvent color. (c),(d) 0.25 M reagents (80 °C, 200  $\mu$ L  
7 flowrate and  $t_R = 2$  min).

14  
15 Initially, 35  $\mu$ m KCl seed crystals are created using dry sieving. These sieved seeds are weighed,  
16 suspended in the solvent, and delivered into the reactor with the base. The effect of increasing the  
17 crystal seed amount on reactor clogging is determined by the pressure increase inside the reactor.  
18 A rapid increase in pressure is indicative of clogging and the interruption of flow. As an initial  
19 study, we perform an acid-base reaction with and without seed crystals, with benzoyl chloride as  
20 the acid and potassium tert-pentoxide as the base (**Table 1**). Without any seed crystals, the pressure  
21 drop increases rapidly and the reactor clogs within 5 reactor volumes (**Supplementary Figure**  
22 **S1a**). Adding 0.05 and 0.10 mg/mL seed crystals extends the reactor lifetime to 8 and 15+ reactor  
23 volumes, respectively. However, when the initial seed loading is increased to 0.2 mg/mL, reactor  
24 clogging occurs within 8 reactor volumes. These data suggest that an optimal seed loading  
25 concentration is necessary to extend reactor lifetime.

KCl Seed Concentration (mg/mL)	Reactor Volumes Until Clog	
	Average	Std. Dev.
0	4.8	0.3
0.05	8.0	
0.1	16.5	3.5
0.2	7.2	1.2

**Table 1: Reactor volumes until clogging occurs during 0.1 M acid-base reaction in a small scale reactor (at 62.5  $\mu\text{L}/\text{min}$  and room temperature,  $t_R = 4$  min). Addition of 35  $\mu\text{m}$  KCl seeds extends reactor lifetime. An optimal amount of seed addition exists at 0.1 mg/mL.**

The Pd-catalyzed amination of aniline and 4-chloroanisole is carried out next to study the effect of KCl seed loading on reactor clogging behavior on a pharmaceutically relevant reaction, at a concentration of 0.25 M and 70  $^{\circ}\text{C}$ , at a flowrate of 90  $\mu\text{L}/\text{min}$  (Residence time ( $T_R$ ) = 4 min). In the control reaction, without the seeds, the reactor clogs within 4 residence volumes (**Table 2, Supplementary Figure S1b**). A seed loading of 0.05 mg/mL is found to extend the lifetime of the reactor by a factor of 2.5. However, when the seed loading is increased to 0.1 mg/mL, the reactor clogs within 5 reactor volumes. These results indicate that an optimal seed loading is required to prevent clogging and extend the reactor lifetime. It is possible that because of the large initial seed crystal size, a dense initial suspension can promote clogging.

KCl Seed Concentration (mg/mL)	Reactor Volumes Until Clog	
	Average	Std. Dev.
0	3.5	0.7
0.05	9.6	5.3
0.1	4.8	

**Table 2: Reactor volumes until clogging occurs during a Pd-catalyzed amination reaction, with reaction conditions of 90  $\mu\text{L}/\text{min}$  and 70  $^{\circ}\text{C}$ . Seeds were 35  $\mu\text{m}$  or smaller. Addition of 35  $\mu\text{m}$  KCl seeds extends reactor lifetime. An optimal amount of seed addition exists at 0.05 mg/mL.**

Next, we use smaller seeds so that the KCl formed during the reaction would be presented with a larger surface area for crystal growth, while keeping the seed mass (and volume) constant. In order

1  
2  
3 to reduce the size of seed crystals added into the reagent, we use a 5  $\mu\text{m}$  syringe filter to obtain  
4 seed crystals with an upper size of 5  $\mu\text{m}$ . The mass of the crystallites present in the filtered  
5 suspension cannot be easily measured as it is impossible to resuspend the seed crystallites after  
6 drying the sample completely. Therefore, an optical counting method is used to measure the  
7 concentration of the seed crystallites. Crystals smaller than 2  $\mu\text{m}$  cannot be counted using this  
8 method, leading to an undercounting of seed loading. Using this lower bound of the seed crystal  
9 concentration, we study the effect of the seed crystals on the Pd-catalyzed amination of aniline and  
10 4-chloroanisole, at a concentration of 0.25 M and 90  $^{\circ}\text{C}$ , with a flowrate of 200  $\mu\text{L}/\text{min}$  ( $t_{\text{R}} = 2$   
11 min). **Table 3** and **Supplementary Figure S1c** shows the result of adding smaller seed crystals.  
12 The control reaction clogs the reactor within 5 reactor volumes, while the reaction with 100,000  
13 seed crystals/mL shows no clogging for the duration of the reaction in all cases. This result further  
14 validates our hypothesis that adding seed crystals causes the KCl formed during reaction to grow  
15 compactly on the seed crystals, resulting in fewer clogging events. However, syringe filtration of  
16 KCl crystals is a slow and cumbersome process and cannot be easily scaled for industrial  
17 production.  
18  
19  
20  
21  
22  
23  
24  
25  
26  
27  
28  
29  
30  
31  
32  
33  
34  
35  
36  
37

	KCl Seed Concentration (Crystals/mL)	Reactor Volumes Until Clog	
		Average	Std. Dev.
Control	0	5.0	0.6
Filtration	$1 \times 10^5$	14.4*	5.3
Settling	$9.3 \times 10^6$	12.2	4.0

38  
39  
40  
41  
42  
43  
44  
45  
46  
47  
48 **Table 3: Reactor volumes until clogging occurs during a Pd-catalyzed amination reaction at**  
49 **reaction conditions of 200  $\mu\text{L}/\text{min}$  and 80  $^{\circ}\text{C}$ . Seeds were 5  $\mu\text{m}$  or smaller when isolated by**  
50 **filtration and counted using optical techniques, or 7  $\mu\text{m}$  or smaller, when isolated by settling**  
51  
52  
53  
54  
55  
56  
57  
58  
59  
60

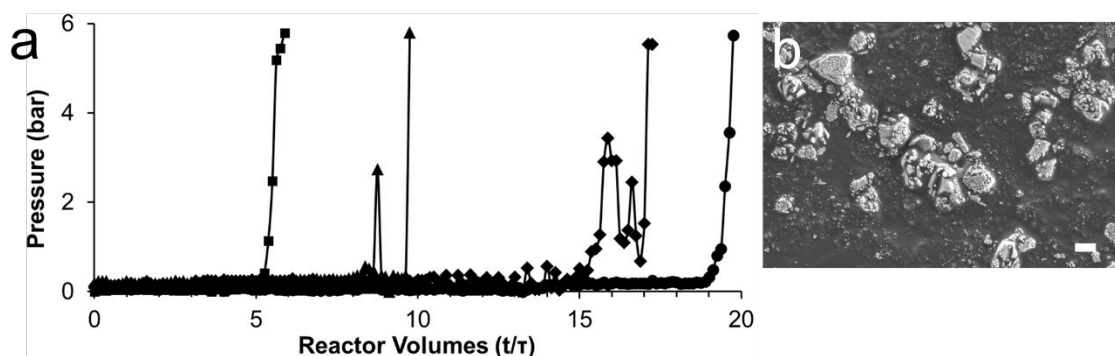
1  
2  
3 **and counted using scanning electron microscopy. \*No clogging occurred when the filtered**  
4 **seeds were used, and the reaction was run until starting materials were used completely.**  
5  
6

7  
8 Settling is an easier method of creating seed crystals of a similar size range as the filtered crystals.  
9  
10 After dry sieving the crystallites with a mesh filter of 35  $\mu\text{m}$ , the KCl seeds are suspended in the  
11 solvent, and allowed to settle. The settling velocity of different sized KCl crystallites can be  
12 calculated as  
13  
14  
15

$$w = \frac{g(\rho_p - \rho)D_p^2}{18\mu} \quad (1)$$

16  
17  
18 Here  $w$  is the settling velocity,  $g$  is gravitational acceleration,  $\rho_p$  is the KCl density,  $\rho$  is the solvent  
19 density,  $D_p$  is the KCl seed crystal diameter, and  $\mu$  is the solvent viscosity. Crystallites smaller than  
20  
21  
22  
23  
24  
25  
26  
27  
28  
29  
30  
31  
32  
33  
34  
35  
36  
37  
38  
39  
40  
41  
42  
43  
44  
45  
46  
47  
48  
49  
50  
51  
52  
53  
54  
55  
56  
57  
58  
59  
60

7  $\mu\text{m}$  are obtained and concentrated by drying the mTHF using an argon stream. The seed crystal size distribution with a lower limit of 100 nm is measured using scanning electron microscopy (SEM) (**Figure 3b**). The size distribution of the KCl seed crystals show the majority of the crystallites are smaller than 1  $\mu\text{m}$ , below the optical counting limit of conventional optics based particle counters (**Supplementary Figure S2**).



1  
2  
3 **Figure 3: (a) Pressure drop data showing clogging behavior. Reaction with  $< 7 \mu\text{m}$  sized**  
4 **seeds,  $9.3 \times 10^6$  seeds/mL, counted using SEM (at  $200 \mu\text{L}/\text{min}$  and  $80 \text{ }^\circ\text{C}$ ). The mixing region**  
5 **before the reagents reach the reactor are sonicated to ensure that seeds do not settle at the**  
6 **start of the reaction. However, clogging occurs at 20 reactor volume (80 min) in the system**  
7 **without reaction. Legend: -■- Control, -▲- Control with sonication, -◆-  $9.3 \times 10^6$  Seed**  
8 **crystals/mL, -●- Reactants without catalyst (i.e., no reaction). (b) SEM images of KCl seed**  
9 **crystals obtained by using the settling method. Scale bar is  $2 \mu\text{m}$ .**

10  
11  
12  
13  
14  
15  
16  
17  
18  
19  
20 Model predictions provide insight into the impact of different seed crystals on the surface area  
21 available for KCl deposition, and the possible maximum amount of KCl deposition onto the  
22 crystals (**Figure 4**). Dry sieved crystals have a larger initial size ( $< 35 \mu\text{m}$ ), which results in a low  
23 count of seeds ( $\sim 600$  crystals/mL) that can be added into the reagent stream before the seeds  
24 promote faster clogging, which also means a low initial surface area for KCl deposition  
25 (**Supplementary Table S1**). The low initial surface area and the low crystal count limits the total  
26 KCl that can be deposited onto the seed crystals, as the crystal deposition rate scales linearly with  
27 both crystal count and surface area.  
28  
29  
30  
31  
32  
33  
34  
35  
36  
37  
38  
39  
40  
41  
42  
43  
44  
45  
46  
47  
48  
49  
50  
51  
52  
53  
54  
55  
56  
57  
58  
59  
60

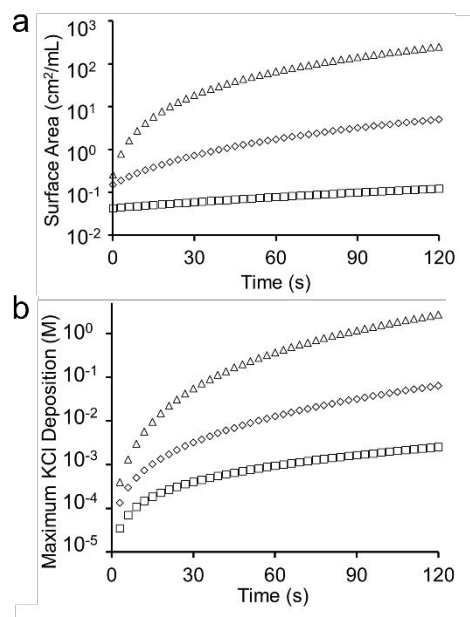


**Figure 4: (a) Seed crystal surface area evolution assuming 0.1  $\mu\text{m/s}$  growth rate. (b) Potential KCl deposition possible on seed crystals assuming 0.1  $\mu\text{m/s}$  crystal growth rate. Legend:  $\square$  Dry Sieved Seeds,  $\diamond$  Filtered Seeds,  $\Delta$  Settled Seeds.**

When the seed crystals are created using filtration and are counted optically, the initial surface area available for KCl deposition increases by a factor of three (**Supplementary Table S1**). More importantly,  $\sim 100,000$  crystals/mL filtered seed crystals can be added without clogging, instead of  $\sim 1,000$  crystals/mL of dry sieved seed crystals. However, if the reaction is completed in a short residence time ( $t_R = 2$  min), only 25 % of the KCl produced during a 0.25 M reaction can be deposited onto the seed crystals due to a lack of surface area.

If the settling method is used and the seed crystals are accurately counted using SEM, the seed crystal concentration can be increased to 6 - 10 million crystals/mL, with an average initial size of 800 nm. The full amount of KCl formed during the reaction can be potentially deposited onto these seed crystals, even at short residence times ( $t_R = 2$  min). The relation between surface area present

1  
2  
3 for crystal growth and the uptake potential of the seed crystals in the 3 methods of seed preparation  
4 is represented in **Figure 4**, assuming a  $0.1 \mu\text{m/s}$  KCl crystal growth rate. This growth rate was  
5  
6 chosen because it theoretically yields crystals of similar size to the final crystallites observed in  
7  
8 SEM images.  
9  
10

11  
12  
13 The seed crystals obtained through settling are added to the Pd-catalyzed amination of aniline and  
14  
15 4-chloroanisole at a concentration of 0.25 M and  $80 \text{ }^\circ\text{C}$ , with a flowrate of  $200 \mu\text{L/min}$  ( $t_R = 4$   
16  
17 min). **Figure 3** shows that with  $\sim 9 \times 10^6$  seed crystals/mL clogging occurs at 17 reactor volumes  
18  
19 (68 min), while the control systems without or with sonication at the mixing region clogs at 5 and  
20  
21 10 reactor volumes, respectively. Importantly, the clogging of the seeded reactor occurs at the  
22  
23 mixing region, and not the reactor itself. To explore why the mixing region clogs, a control was  
24  
25 run without any seeds or catalyst. This reaction stream still clogs at the mixing region within 20  
26  
27 reactor volumes (**Figure 3**). X-ray diffraction (XRD) of the unreacted, mixed reagent stream  
28  
29 showed the existence of potassium hydroxide, which indicates that there is water present in the  
30  
31 system that reacts with the potassium tert-butoxide and forms KOH in the mixer (**Supplementary**  
32  
33 **Figure S3**).

34  
35  
36 We hypothesize that without seed addition, the supersaturation profile that develops during the  
37  
38 reaction causes the formation of numerous small crystallites, due to the formation of large amounts  
39  
40 of the byproduct in a solvent with a low solubility. Due to the rapid formation of these crystallites,  
41  
42 we observe dendritic growth. These uncontrolled crystal nucleation events give rise to a non-  
43  
44 compact morphology. Although both compact and non-compact crystal morphologies  
45  
46 (**Supplementary Figure S4**) are created in the unseeded reactor, we hypothesize that the larger  
47  
48 surface area of the dendritic morphologies enable interactions between separate particles, and  
49  
50 allow for the formation of larger multi-crystalline aggregates.<sup>43</sup> These aggregates, in turn, have a  
51  
52  
53  
54  
55  
56  
57  
58  
59  
60

1  
2  
3 slower velocity compared to the surrounding fluid due to their mass, enabling more particle  
4 aggregation until a clog is created in the reactor.  
5  
6

7  
8 On the other hand, when an optimized amount of crystalline seeds are added into the reactor, the  
9 crystal surface allows for crystal growth, instead of just nucleation of numerous crystallites as in  
10 the unseeded reactor. As the nucleation rate is a strong function of supersaturation, a small decrease  
11 in supersaturation can have a strong impact on the nucleation rate.<sup>44</sup> Thus, the reduction of new  
12 crystallites and the growth of seeds, lead to the formation of more compact structures than the  
13 dendritic aggregates seen in the unseeded case. The compact structures reduce clogging events, as  
14 multi particle aggregation becomes less likely.  
15  
16  
17  
18  
19  
20  
21  
22  
23

24  
25 The high concentrations of salt produced during the reaction allows for roughened growth on the  
26 seed surface. Thus, it is possible for these surface to serve as secondary nucleation sites as well.  
27  
28 However, we show that even less compact seed morphologies, like that of NaBr (Supplementary  
29 Figure S6), can reduce the clogging issues when a NaBr producing C-N bond formation reaction  
30 is used (Supplementary Figure S7). Therefore, we also show that the seed crystal method is  
31 effective on other Pd-catalyzed amination reactions that produce chemically different salt  
32 byproducts such as NaBr (**Supplementary Figures S5-S7**).  
33  
34  
35  
36  
37  
38  
39  
40  
41

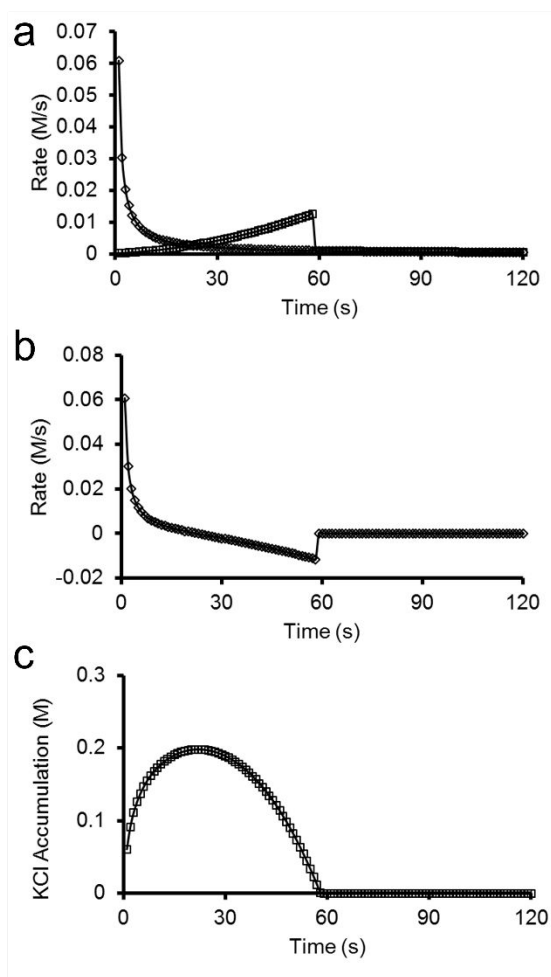
42 A priori prediction of the optimum concentration is difficult, as many factors can influence  
43 the crystallization kinetics, including the reactor type, temperature, flow rate, crystal structure, and  
44 any morphological modification that the reactants or products/byproducts may cause. However,  
45 the modelling performed here balances the formation and deposition rates for a given reaction and  
46 byproduct, and can thus be used to optimize seed size and loadings for different concentrations  
47 and temperatures for the same reaction.  
48  
49  
50  
51  
52  
53  
54  
55  
56  
57  
58  
59  
60

1  
2  
3 The kinetics of KCl production and deposition on seed crystals were modelled to obtain insights  
4 into the clogging behavior. The KCl production rate was quantified based on experiments  
5  
6 (Supplementary Figure S8). The KCl deposition rate is the rate at which the produced KCl is  
7  
8 absorbed onto the surface of the seed crystals, modeled by assuming a linear growth rate of the  
9  
10 KCl crystals ( $0.1 \mu\text{m/s}$ ) at full KCl saturation (more details in S1 of Supplementary Information).  
11  
12  
13

14  
15 **Figure 5a** shows the relationship between the KCl production rate and the deposition rate during  
16 the residence time of the fluid in the reactor. The KCl production rate decreases over time, as  
17 reactants are consumed. On the other hand, the KCl deposition rate increases over time, as the seed  
18 crystals grow larger (leading to a larger surface area), while the linear growth rate remains  
19 constant. This creates a temporal mismatch between the production and deposition rate, and the  
20 difference leads to an initial accumulation of KCl in the reactor. The KCl accumulation peaks at  
21 25 seconds, when KCl production rate equals the deposition rate (**Figure 5b,c**). Beyond 25  
22 seconds, the excess amount of KCl gradually dwindles as the KCl deposition rate outweighs the  
23 KCl generation rate, until the accumulated KCl is completely consumed at 60 seconds. After 60  
24 seconds, the KCl deposition rate should simply match the KCl generation rate, so that the  
25 incremental amount of KCl generated at this point is instantaneously absorbed by the seed crystals.  
26  
27 In summary, before 60 seconds, the KCl deposition is the rate-limiting step for crystal growth, and  
28 after 60 seconds, the KCl generation becomes the rate-limiting step for crystal growth.  
29  
30  
31  
32  
33  
34  
35  
36  
37  
38  
39  
40  
41  
42  
43  
44  
45

46 Our simulation results also indicate how the seed crystals can be utilized to achieve better results  
47 to avoid clogging. Namely, it is best to match the KCl production rates with the KCl deposition  
48 rates so that the amount of excess KCl built up in the interim is minimized. Rate matching can be  
49 accomplished by several methods: (1) We could slow down the reaction rate, but it is not advisable  
50 to do so as the production of product is stoichiometric with the KCl production; (2) We could  
51  
52  
53  
54  
55  
56  
57  
58  
59  
60

1  
2  
3 increase the total amount of seed crystals, but there is also an upper limit, as too much seed crystals  
4 alone can cause clogging; (3) It is also possible to optimize the seed crystal addition by injecting  
5 progressively into the reaction stream at different concentrations; (4) Finally, external additives  
6 that limit crystal aggregation can be investigated.<sup>45</sup>  
7  
8  
9  
10  
11  
12  
13  
14  
15  
16  
17



18  
19  
20  
21  
22  
23  
24  
25  
26  
27  
28  
29  
30  
31  
32  
33  
34  
35  
36  
37  
38  
39  
40  
41  
42  
43  
44  
45  
46  
47  
48  
49 **Figure 5: (a) Modelling KCl production rate and deposition rate. Production rate matches**  
50 **the deposition rate at 25 s. Legend: -◇- KCl production rate, -□- KCl deposition rate (b)**  
51 **Difference of production and deposition rates. All accumulated KCl can be deposited on the**  
52  
53  
54  
55  
56  
57  
58  
59  
60

1  
2  
3 **crystals by 60 s. (c) KCl accumulation in the reactor based on the production and deposition**  
4 **rates.**  
5  
6

7  
8 **Conclusion:**  
9

10  
11 In this work, we show that crystal growth control in flow chemistry could extend the continuous  
12 flow reactor lifetime compared to the unseeded reactors. Preliminary experiments with an acid  
13 base salt formation reaction showed extended reactor lifetimes without clogging. For the C-N bond  
14 forming reaction, as higher reagent concentrations were desired, larger seed crystals surface area  
15 was required while still minimizing the total volume of seed crystals added. In order to do this,  
16 better techniques of obtaining smaller seed crystals (sieving and settling) as well as better  
17 techniques for counting seeds (SEM based particle counting) were utilized.  
18  
19  
20  
21  
22  
23  
24  
25  
26  
27

28 It was observed that reactions that form stoichiometric amounts of solids could have their crystal  
29 morphology shifted to a compact form instead of fractal-like agglomerates. Different methods of  
30 seed crystal formation and seed crystal counting were explored. Settling the crystal seeds and  
31 counting using SEM were most useful in measuring seed crystal concentration accurately.  
32  
33  
34  
35  
36  
37  
38  
39  
40  
41  
42  
43  
44  
45  
46  
47  
48  
49  
50  
51  
52  
53  
54  
55  
56  
57  
58  
59  
60

Theoretical calculations on solid production and deposition rates showed that clogging could be mitigated by the use of smaller crystals, such that each crystallite could grow to have a larger surface area without an initial increase in solid mass, or by slowing the reaction rate such that the crystals could grow to have a larger surface area for KCl deposition.

Ultrasonication is a more general method of limiting clogging, since it can be utilized when non-crystalline materials (such as polymers) cause clogging, as well as when multiple crystalline byproducts are created within one reactor. However, ultrasonication based de-clogging systems

1  
2  
3 have their own difficulty. In particular, continuous sonication has been shown to change the  
4  
5 kinetics of reactions due to localized temperature increases.<sup>12</sup>  
6  
7

8  
9 The proposed crystal engineering technique can work in conjunction with sonication techniques  
10  
11 to extend reactor lifetimes. As clogging is most likely to occur in narrow junctions, it is possible  
12  
13 to sonicate bends and narrowed regions of the reactor to ensure no clogging occurs.<sup>46</sup> On the other  
14  
15 hand, over long, continuous reactors of constant diameter, it is less feasible to sonicate the entire  
16  
17 reactor. However, as crystallization and aggregation is a stochastic mechanism, there is a  
18  
19 possibility of clogging occurring in this region. We envision the crystal engineering technique  
20  
21 described here to reduce clogging in this reactor region.  
22  
23  
24

25  
26 Crystal engineering can also be useful if further modification of the byproduct or the product is  
27  
28 necessary. For example, the concepts developed here can be utilized to crystallize the product  
29  
30 itself, providing an easy in-line purification and separation technique. With the ease of forming  
31  
32 and adding seed crystals, this method could become a tool alongside sonication, oscillating flows,  
33  
34 and pressure pulses to mitigate clogging effects of salt forming reactions in microfluidic and small-  
35  
36 scale reactors.  
37  
38  
39

#### 40 **Acknowledgement**

41  
42 This work was supported by the Novartis-MIT Center for continuous manufacturing  
43  
44  
45

#### 46 **Conflict of Interest Disclosure:**

47  
48  
49 The authors declare no competing financial interest.  
50  
51  
52  
53  
54  
55  
56  
57  
58  
59  
60

1  
2  
3 **Supplementary information description:**  
4

5  
6 S1. Methodology of KCl Simulation  
7

8  
9 Figure S1: Pressure drop traces showing clogging behavior.  
10

11  
12 Figure S2: Crystal size distribution of settled seeds measured using SEM.  
13

14  
15 Figure S3: X-ray diffraction of reagents and products.  
16

17  
18 Figure S4: SEM of unseeded reactor final crystal morphology.  
19

20  
21 Figure S5: Second Pd-catalyzed C-N bond formation reaction scheme with sodium bromide as  
22 salt byproduct.  
23

24  
25 Figure S6: Sodium bromide (NaBr) seed crystals made through sieving, imaged using SEM.  
26

27  
28 Figure S7: Pressure drop for NaBr producing reaction.  
29

30  
31 Figure S8: Conversion of reaction used to simulate reaction rate.  
32

33  
34 Table S1: Seed crystal characteristics.  
35  
36  
37  
38  
39  
40  
41  
42  
43  
44  
45  
46  
47  
48  
49  
50  
51  
52  
53  
54  
55  
56  
57  
58  
59  
60

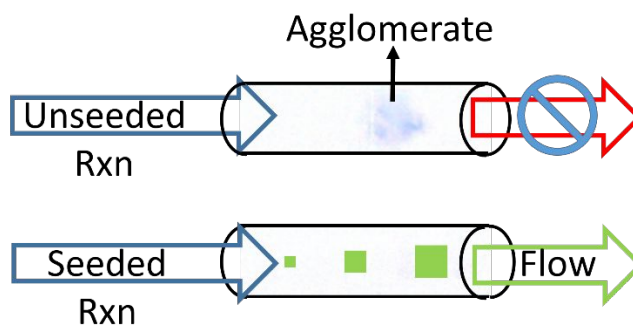
**References:**

- (1) Jensen, K. F., Flow chemistry. Microreaction technology comes of age. *AIChE J.* **2017**, 63, (3), 858-869.
- (2) Gutmann, B.; Cantillo, D.; Kappe, C. O., Continuous-Flow Technology A Tool for the Safe Manufacturing of Active Pharmaceutical Ingredients. *Angew. Chem. Int. Ed.* **2015**, 54, (23), 6688-6728.
- (3) Movsisyan, M.; Delbeke, E. I. P.; Berton, J. K. E. T.; Battilocchio, C.; Ley, S. V.; Stevens, C. V., Taming hazardous chemistry by continuous flow technology. *Chem. Soc. Rev.* **2016**, 45, (18), 4892-4928.
- (4) Ley, S. V.; Fitzpatrick, D. E.; Ingham, R. J.; Myers, R. M., Organic Synthesis: March of the Machines. *Angew. Chem. Int. Ed.* **2015**, 54, (11), 3449-64.
- (5) Ingham, R. J.; Battilocchio, C.; Fitzpatrick, D. E.; Sliwinski, E.; Hawkins, J. M.; Ley, S. V., A Systems Approach towards an Intelligent and Self-Controlling Platform for Integrated Continuous Reaction Sequences. *Angew. Chem. Int. Ed.* **2015**, 54, (1), 144-148.
- (6) Hessel, V.; Kralisch, D.; Kockmann, N.; Noel, T.; Wang, Q., Novel Process Windows for Enabling, Accelerating, and Uplifting Flow Chemistry. *ChemSuschem* **2013**, 6, (5), 746-789.
- (7) Plutschack, M. B.; Pieber, B.; Gilmore, K.; Seeberger, P. H., The Hitchhiker's Guide to Flow Chemistry. *Chem. Rev.* **2017**, 117, (18), 11796-11893.
- (8) Roberge, D. M.; Ducry, L.; Bieler, N.; Cretton, P.; Zimmermann, B., Microreactor Technology: A Revolution for the Fine Chemical and Pharmaceutical Industries? *Chemical Engineering & Technology* **2005**, 28, (3), 318-323.
- (9) Honda, T.; Miyazaki, M.; Nakamura, H.; Maeda, H., Controllable polymerization of N-carboxy anhydrides in a microreaction system. *Lab on a Chip* **2005**, 5, (8), 812-818.
- (10) Li, W.; Pham, H. H.; Nie, Z.; MacDonald, B.; Güenther, A.; Kumacheva, E., Multi-Step Microfluidic Polymerization Reactions Conducted in Droplets: The Internal Trigger Approach. *Journal of the American Chemical Society* **2008**, 130, (30), 9935-9941.
- (11) Marcati, A.; Serra, C.; Bouquey, M.; Prat, L., Handling of Polymer Particles in Microchannels. *Chemical Engineering & Technology* **2010**, 33, (11), 1779-1787.
- (12) Hartman, R. L.; Naber, J. R.; Zaborenko, N.; Buchwald, S. L.; Jensen, K. F., Overcoming the Challenges of Solid Bridging and Constriction during Pd-Catalyzed C-N Bond Formation in Microreactors. *Organic Process Research & Development* **2010**, 14, (6), 1347-1357.
- (13) Hartman, R. L., Managing Solids in Microreactors for the Upstream Continuous Processing of Fine Chemicals. *Organic Process Research & Development* **2012**, 16, (5), 870-887.
- (14) Bengtsson, M.; Laurell, T., Ultrasonic agitation in microchannels. *Anal Bioanal Chem* **2004**, 378, (7), 1716-1721.
- (15) Přibyl, M.; Šnita, D.; Marek, M., Nonlinear phenomena and qualitative evaluation of risk of clogging in a capillary microreactor under imposed electric field. *Chemical Engineering Journal* **2005**, 105, (3), 99-109.
- (16) Poe, S. L.; Cummings, M. A.; Haaf, M. P.; McQuade, D. T., Solving the Clogging Problem: Precipitate-Forming Reactions in Flow. *Angewandte Chemie International Edition* **2006**, 45, (10), 1544-1548.
- (17) Noel, T.; Naber, J. R.; Hartman, R. L.; McMullen, J. P.; Jensen, K. F.; Buchwald, S. L., Palladium-catalyzed amination reactions in flow: overcoming the challenges of clogging via acoustic irradiation. *Chemical Science* **2011**, 2, (2), 287-290.

- 1  
2  
3 (18) Nagasawa, H.; Mae, K., Development of a New Microreactor Based on Annular  
4 Microsegments for Fine Particle Production. *Industrial & Engineering Chemistry Research*  
5 **2006**, 45, (7), 2179-2186.
- 6 (19) Kuhn, S.; Noel, T.; Gu, L.; Heider, P. L.; Jensen, K. F., A Teflon microreactor with  
7 integrated piezoelectric actuator to handle solid forming reactions. *Lab on a Chip* **2011**, 11, (15),  
8 2488-2492.
- 9 (20) Horie, T.; Sumino, M.; Tanaka, T.; Matsushita, Y.; Ichimura, T.; Yoshida, J.-i.,  
10 Photodimerization of Maleic Anhydride in a Microreactor Without Clogging. *Organic Process*  
11 *Research & Development* **2010**, 14, (2), 405-410.
- 12 (21) Kopach, M. E.; Roberts, D. J.; Johnson, M. D.; McClary Groh, J.; Adler, J. J.; Schafer, J.  
13 P.; Kobierski, M. E.; Trankle, W. G., The continuous flow Barbier reaction: an improved  
14 environmental alternative to the Grignard reaction? *Green Chemistry* **2012**, 14, (5), 1524-1536.
- 15 (22) Huang, X.; Anderson, K. W.; Zim, D.; Jiang, L.; Klapars, A.; Buchwald, S. L.,  
16 Expanding Pd-Catalyzed C–N Bond-Forming Processes: The First Amidation of Aryl  
17 Sulfonates, Aqueous Amination, and Complementarity with Cu-Catalyzed Reactions. *Journal of*  
18 *the American Chemical Society* **2003**, 125, (22), 6653-6655.
- 19 (23) Naber, J. R.; Buchwald, S. L., Packed-Bed Reactors for Continuous-Flow C–N Cross-  
20 Coupling. *Angewandte Chemie* **2010**, 122, (49), 9659-9664.
- 21 (24) Chen, M.; Buchwald, S. L., Continuous-Flow Synthesis of 1-Substituted Benzotriazoles  
22 from Chloronitrobenzenes and Amines in a C–N Bond  
23 Formation/Hydrogenation/Diazotization/Cyclization Sequence. *Angewandte Chemie*  
24 *International Edition* **2013**, 52, (15), 4247-4250.
- 25 (25) Mascia, S.; Heider, P. L.; Zhang, H.; Lakerveld, R.; Benyahia, B.; Barton, P. I.; Braatz,  
26 R. D.; Cooney, C. L.; Evans, J. M. B.; Jamison, T. F.; Jensen, K. F.; Myerson, A. S.; Trout, B.  
27 L., End-to-End Continuous Manufacturing of Pharmaceuticals: Integrated Synthesis,  
28 Purification, and Final Dosage Formation. *Angewandte Chemie International Edition* **2013**, 52,  
29 (47), 12359-12363.
- 30 (26) Mo, Y.; Jensen, K. F., A miniature CSTR cascade for continuous flow of reactions  
31 containing solids. *Reaction Chemistry & Engineering* **2016**, 1, (5), 501-507.
- 32 (27) Chapman, M. R.; Kwan, M. H. T.; King, G.; Jolley, K. E.; Hussain, M.; Hussain, S.;  
33 Salama, I. E.; González Niño, C.; Thompson, L. A.; Bayana, M. E.; Clayton, A. D.; Nguyen, B.  
34 N.; Turner, N. J.; Kapur, N.; Blacker, A. J., Simple and Versatile Laboratory Scale CSTR for  
35 Multiphase Continuous-Flow Chemistry and Long Residence Times. *Organic Process Research*  
36 *& Development* **2017**, 21, (9), 1294-1301.
- 37 (28) Podder, J.; Basu, R.; Evitts, R. W.; Besant, R. W., Surface Morphology and  
38 Microstructural Characterization of KCl Crystals Grown in Halite–Sylvite Brine Solutions by  
39 Electron Backscattered Diffraction Techniques. *Surface Review and Letters* **2015**, 22, (01),  
40 1550012.
- 41 (29) Beckmann, W., Seeding the Desired Polymorph: Background, Possibilities, Limitations,  
42 and Case Studies. *Organic Process Research & Development* **2000**, 4, (5), 372-383.
- 43 (30) Majano, G.; Darwiche, A.; Mintova, S.; Valtchev, V., Seed-Induced Crystallization of  
44 Nanosized Na-ZSM-5 Crystals. *Industrial & Engineering Chemistry Research* **2009**, 48, (15),  
45 7084-7091.
- 46 (31) Yu, Z. Q.; Chow, P. S.; Tan, R. B. H., Seeding and Constant-Supersaturation Control by  
47 ATR-FTIR in Anti-Solvent Crystallization. *Organic Process Research & Development* **2006**, 10,  
48 (4), 717-722.
- 49  
50  
51  
52  
53  
54  
55  
56  
57  
58  
59  
60

- 1  
2  
3 (32) Chung, S. H.; Ma, D. L.; Braatz, R. D., Optimal seeding in batch crystallization. *The Canadian Journal of Chemical Engineering* **1999**, 77, (3), 590-596.
- 4  
5 (33) Fors, B. P.; Watson, D. A.; Biscoe, M. R.; Buchwald, S. L., A Highly Active Catalyst for  
6 Pd-Catalyzed Amination Reactions: Cross-Coupling Reactions Using Aryl Mesylates and the  
7 Highly Selective Monoarylation of Primary Amines Using Aryl Chlorides. *Journal of the*  
8 *American Chemical Society* **2008**, 130, (41), 13552-13554.
- 9  
10 (34) Surry, D. S.; Buchwald, S. L., Dialkylbiaryl phosphines in Pd-catalyzed amination: a  
11 user's guide. *Chemical Science* **2011**, 2, (1), 27-50.
- 12  
13 (35) Surry, D. S.; Buchwald, S. L., Biaryl Phosphane Ligands in Palladium-Catalyzed  
14 Amination. *Angewandte Chemie International Edition* **2008**, 47, (34), 6338-6361.
- 15  
16 (36) Hartwig, J. F., Evolution of a Fourth Generation Catalyst for the Amination and  
17 Thioetherification of Aryl Halides. *Accounts of Chemical Research* **2008**, 41, (11), 1534-1544.
- 18  
19 (37) Kantchev, E. A. B.; O'Brien, C. J.; Organ, M. G., Palladium Complexes of N-  
20 Heterocyclic Carbenes as Catalysts for Cross-Coupling Reactions—A Synthetic Chemist's  
21 Perspective. *Angewandte Chemie International Edition* **2007**, 46, (16), 2768-2813.
- 22  
23 (38) Bruno, N. C.; Niljianskul, N.; Buchwald, S. L., N-Substituted 2-Aminobiphenylpalladium  
24 Methanesulfonate Precatalysts and Their Use in C–C and C–N Cross-Couplings. *The Journal of*  
25 *Organic Chemistry* **2014**, 79, (9), 4161-4166.
- 26  
27 (39) Doki, N.; Kubota, N.; Sato, A.; Yokota, M., Effect of cooling mode on product crystal  
28 size in seeded batch crystallization of potassium alum. *Chemical Engineering Journal* **2001**, 81,  
29 (1–3), 313-316.
- 30  
31 (40) Lin, M. Y.; Lindsay, H. M.; Weitz, D. A.; Ball, R. C.; Klein, R.; Meakin, P., Universality  
32 in colloid aggregation. *Nature* **1989**, 339, (6223), 360-362.
- 33  
34 (41) Meakin, P., Formation of Fractal Clusters and Networks by Irreversible Diffusion-  
35 Limited Aggregation. *Physical Review Letters* **1983**, 51, (13), 1119-1122.
- 36  
37 (42) Lattuada, M.; Sandkühler, P.; Wu, H.; Sefcik, J.; Morbidelli, M., Aggregation kinetics of  
38 polymer colloids in reaction limited regime: experiments and simulations. *Advances in Colloid*  
39 *and Interface Science* **2003**, 103, (1), 33-56.
- 40  
41 (43) Flowers, B. S.; Hartman, R. L., Particle Handling Techniques in Microchemical  
42 Processes. *Challenges* **2012**, 3, (2), 194.
- 43  
44 (44) Vesselinov, M. I., *Crystal growth for beginners: fundamentals of nucleation, crystal*  
45 *growth and epitaxy*. ed.; World scientific: 2016.
- 46  
47 (45) Vagenende, V.; Yap, M. G. S.; Trout, B. L., Mechanisms of Protein Stabilization and  
48 Prevention of Protein Aggregation by Glycerol. *Biochemistry* **2009**, 48, (46), 11084-11096.
- 49  
50 (46) Dressaire, E.; Sauret, A., Clogging of microfluidic systems. *Soft Matter* **2017**, 13, (1), 37-  
51 48.  
52  
53  
54  
55  
56  
57  
58  
59  
60

1  
2  
3 **For Table of Contents Use only:**  
4  
5



18 Adding seed crystals of crystalline byproducts during a continuous flow synthesis promotes the  
19 growth of compact, high quality crystals instead of agglomerates. These compact crystals are less  
20 likely to clog the reactor, extending the reactor lifetime for the carbon-nitrogen bond forming  
21 reaction.  
22  
23  
24  
25  
26  
27  
28  
29  
30  
31  
32  
33  
34  
35  
36  
37  
38  
39  
40  
41  
42  
43  
44  
45  
46  
47  
48  
49  
50  
51  
52  
53  
54  
55  
56  
57  
58  
59  
60